LRP 692/01 March 2001

TCV DNBI Profile and Attenuation Studies with Code Manual

J. Mlynar

ISSN 0458-5895

March 2001

TCV DNBI Profile and Attenuation Studies with Code Manual

J. Mlynar

Abstract:

For absolute measurements using neutral beam in high temperature plasmas a reliable model on the beam profile and intensity is necessary. Within this report we study the case of neutral hydrogen beam in plasmas of tokamak TCV. Appropriate approximations for the beam profile and attenuation are derived and the corresponding MatLab code package is thoroughly explained. Several examples of the model results are presented.

Contents:

1. Introduction

In 2000, a diagnostic beam neutral injector (DNBI) from Budker's Institute of Nuclear Physics (BINP, Novosibirsk) has been commissioned at TCV [1]. The neutral beam provided by the DNBI has the following characteristics:

- beam energy range: 20-50 keV (optimized for 50 keV),
- equivalent beam current: 0.5 A at 50 keV within ϕ 10 cm diameter in the beam focus,
- modulation: on-time range 1 ms to 2 s, minimal off-time 2 s,
- beam focus near the centre of the TCV plasma, beam divergence 0.6-0.7°,
- beam components: 73% H_1^+, 20% H_2^+ and 7% H_3^+ in beam source electrical current.

The principal scheme of the injector is outlined in Fig. 1. The prior task of the DNBI is to provide hand in hand with CXRS (Charge eXchange Recombination Spectroscopy, see Fig. 3) a diagnostic tool for the local measurement of the TCV plasma ion temperature [1].

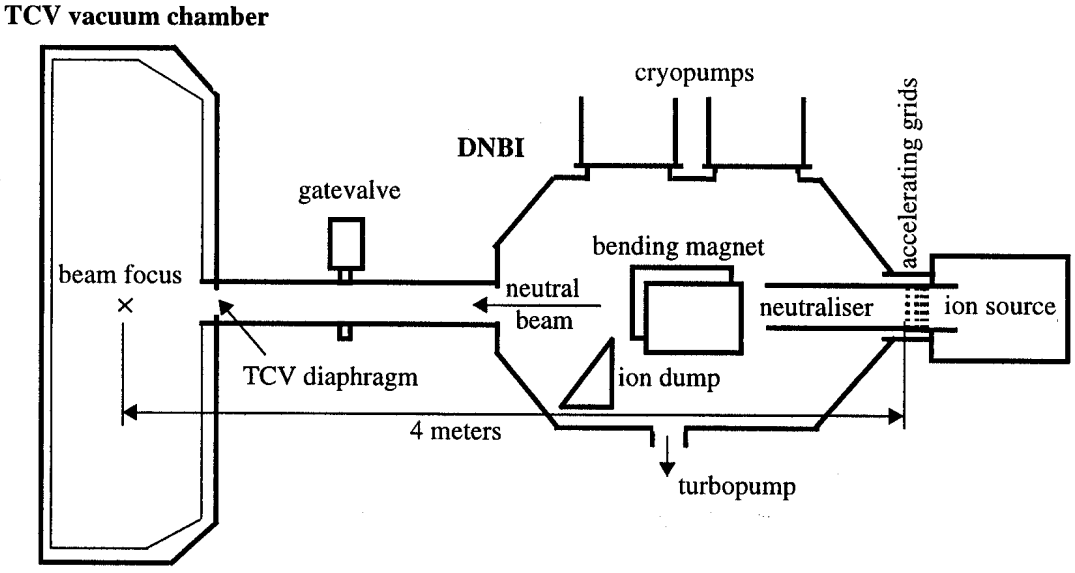

***Figure 1:** Schematic setup of diagnostics neutral beam injector at TCV*

However, diagnostic beams can deliver further information on plasma characteristics along the beam path [2]. Obviously, for all absolute measurements using DNBI the beam local intensity (its current density) has to be known. For example, if the CXRS diagnostic is absolutely calibrated, it is possible to measure the local density of impurities provided the local beam neutral current density is known. The task is complicated by the fact that the beam attenuation depends in return on the impurity concentration. Within this report we introduce a starting point: simple approximations for beam profile and attenuation evaluation using only standard, beam independent TCV data. A modular code package is presented which applies these principles and which can be easily extended to integrate new measurements, including the data from CXRS diagnostics itself.

1. Tokamak à Configuration Variable, R = 0.88 m, a < 0.25 m, with extended capabilities of plasma shaping and positioning, for details see http://crppwww.epfl.ch/tcv/parameters.htm

A simple yet quite precise approximation formula for the beam profile in vacuum (no beam attenuation) is derived in section 2. Second, quantitative consequences of the ratio of beam components presented above are discussed in section 3. An approximation for the beam attenuation in plasma is presented in section 4. It has been optimized so that it benefits from experimental data available on TCV but needs no further plasma modelling.

The section 5 describes in detail a package of MatLab codes which applies the above reported formulas and principles. The section provides a brief user's manual for the code package. In the section 6 we present some of the most representative results of the calculations. Resulting beam current densities in vacuum as well as in real TCV shots are outlined. A short discussion on the present state and future applications of the model concludes this report.

2. Beam profile

In order to evaluate the beam intensity at any point in the plasma it is essential to know the vacuum beam profile. We shall model it in a cylindrical geometry, with the origin of the axis at the accelerating grid. As follows from the beam source geometry, the beam is axially symmetric so that we shall describe the beam profile in terms of particle current density as a function of z (distance from the grid) and r (distance from the beam axis). Thanks to the spherically shaped accelerating grid each beam particle is accelerated to a speed v_b towards the focus (the center of the sphere) which is at a distance z_{foc}. The particles have also finite perpendicular velocity v_t due to their thermal motion (at temperature T_b) and due to stray electrical fields at accelerating grids, therefore the beam suffers dispersion which results in its non-zero width at the focus.

Let us suppose that the beam source is homogeneous so that the beam can be divided into identical elementary filaments, each being emitted by an elementary source surface dS. Next, suppose that the beam particles' perpendicular velocities have thermal distribution, so that each filament evolves into a Gaussian with distance from the source. As all the filaments intersect in the beam focus, the beam profile at that point correspond to a trivial sum of the coaxial elementary Gaussians which results in the form

$$j(z = z_{foc}, r) = g(z)\,exp\left(-\frac{\alpha r^2}{z^2}\right) \qquad \text{(Eq. 1)}$$

where $\alpha = \frac{v_b^2}{\langle v_t^2 \rangle} \approx \frac{E_b}{T_b}$ and E_b is the nominal (full) beam energy. At this point we can determine the function $g(z)$ from the simple fact that the total beam current must not be dependent on the z coordinate:

$$I = 2\pi \int_0^\infty j(z, r) r dr = const \qquad \text{(Eq. 2)}$$

which gives

$$g(z) = \frac{I\alpha}{\pi z^2} \qquad \text{(Eq. 3)}$$

Beyond the focus, however, the resulting beam profile has to be calculated as a convolution of elementary Gaussians with the source image $Q(r, \varphi, z) = \frac{Q(r, \varphi)}{1 - z/z_{foc}}$, where $Q(r, \varphi)$ describes the source function (normalized current density) at the accelerating grid:

$$j(z, r) = g(z) exp\left(-\frac{\alpha r^2}{z^2}\right) * Q(r, \varphi) = \qquad \text{(Eq. 4)}$$

$$= g(z) \int_0^{\infty} \int_0^{2\pi} exp\left(-\alpha \frac{r^2 - 2r\tilde{r}(1 - z/z_{foc}) cos(\tilde{\varphi} - \varphi) + \tilde{r}^2(1 - z/z_{foc})}{z^2}\right) Q(\tilde{r}, \tilde{\varphi}) \tilde{r} d\tilde{r} d\tilde{\varphi}$$

Next we shall neglect the fact that the source consist of 163 beamlets and consider a homogeneous, constant current density source:

$$Q(r, \varphi) = \frac{1}{\pi a^2} \qquad r \le a$$

$$Q(r, \varphi) = 0 \qquad r > a$$

then from (Eq. 4) one can get the beam profile:

$$j(z, r) = \frac{g(z)}{\pi a^2} exp\left(-\frac{\alpha r^2}{z^2}\right) \int_0^a exp\left(-\frac{\alpha \tilde{r}^2}{z^{*2}}\right) \underbrace{\int_0^{2\pi} exp\left(\frac{2r\tilde{r} cos\tilde{\varphi}}{z|z^*|}\right) d\tilde{\varphi}}_{2\pi I_0\left(\frac{2r\tilde{r}}{z|z^*|}\right)} \tilde{r} d\tilde{r} \qquad \text{(Eq. 5)}$$

where $\frac{1}{z^*} = \frac{1}{z} - \frac{1}{z_{foc}}$ and I_0 is the modified Bessel function of the first kind, zero order. The absolute value reflects the fact that with changing the sign of z^*, the sign of $cos\varphi$ also changes. The function $g(z)$ is given by (Eq. 3).

Notice that the local current density $j(z,r)$ is to be determined by integration of a nontrivial function even though a simplified model of constant homogenous source has been considered. This is an undesirable feature, because in the beam profile modelling we will need a fast evaluation of the whole function $j(z, r)$. An approximation would be however sufficient if it corresponds well to the convolution formula at least within the plasma, i.e. not far from the focus z_{foc}.

Quite naturally the starting point in the search for an approximation is (Eq. 1), which gives a very simple rule for the beam profile in the focus. We shall suppose that an exponential profile will suit also in the focus vicinity. That is, we assume that the result is to be found in form

$$j(z, r) = C_1(z) exp(-C_2(z) r^2)$$

The coefficient $C_1(z)$ equals to the on-axis current $j(z, r = 0)$ which can be easily found from convolution formula (Eq. 5) and (Eq. 3):

$$j(z,0) = \frac{I}{\pi a^2}\frac{z^{*2}}{z^2}\left(1 - exp\left(-\frac{\alpha a^2}{z^{*2}}\right)\right) \qquad \text{(Eq. 6)}$$

The coefficient $C_2(z)$ is then found so that the resulting equation fulfils the current conservation (Eq. 2). This way we get:

$$j(z,r) = j(z,0)\cdot exp\left(-\frac{\pi}{I}j(z,0)\cdot r^2\right) \qquad \text{(Eq. 7)}$$

Notice that indeed

$$\lim_{z \to z_{foc}} j(z,0) = \frac{I\alpha}{\pi z^2} \qquad \text{(Eq. 8)}$$

Instead of the beam diffusion coefficient α the beam divergence ϑ,

$$tan\vartheta = 1/\sqrt{\alpha} \qquad \text{(Eq. 9)}$$

is usually used in practice. Its value for our DNBI is $\vartheta \cong 0.6° - 0.7°$. The three beam components can be easily introduced by distinguishing three beam currents I_E, $I_{E/2}$ and $I_{E/3}$, see section 3.

The difference in between the above formulae (Eq. 6) & (Eq. 7) and the full convolution model (Eq. 5) has been found to be negligible within the TCV vessel (below 10^{-6} for $z - z_{foc} < 0.3$ m). In other words, the beam profile can be considered exponential along its path in the plasma, which saves a lot of computing. Anyway, more important irregularities of the gaussian profile are supposed to occur due to more complex reasons, namely due to the perpendicular stray fields in between accelerating grids which result in irregular non-maxwellian beam dispersion, see [3].

Yet more simplified formula, corresponding to (Eq. 1), would be obtained under the supposition that the ion source dimensions are negligible. Still we have preferred to apply the (Eq. 7) which is much more precise and does not make any noticeable difference in the computing time. A more important computing load follows anyway from the fact that the beam source visibility through the port diaphragm must be evaluated, see section 5.1.

The beam "halo" is another important effect which aplifies the beam profile width and intensity, though at a different energy of neutrals. It is formed by the secondary, thermal neutrals in the beam vicinity and originates as fall-out of the charge exchange between the beam and plasma particles. Therefore, it represents a quite complicated, plasma-dependent phenomena which may pose a considerable computer load if treated in detail. The energy spectrum of the beam halo neutrals correspond to plasma ion temperature, which is considerably lower than the beam energy. Consequently, the beam halo influences less the optical observations than the UV observations. Within this study the effect of beam "halo" has not been considered, but the coding is flexible enough to assume this effect at a later stage, see section 5. The expected influence of the beam halo on the CX spectra is in order of ten percent so that the effect should be eventually introduced at least as a fixed correction profile [4].

3. Beam components

According to the supplier the ion beam extracted from the DNBI ion source consists of approx. 73% H_1^+, 20% H_2^+ and 7% H_3^+ in electrical current. All the components are single-charged, so that the same ratio holds for the particle flux before their dissociation. The three components get the same energy during acceleration but they differ in their mass as $1 : 2 : 3$, so that their velocity goes as $1 : 1/\sqrt{2} : 1/\sqrt{3}$. The consecutive hydrogen gas neutraliser is "thick", i.e. almost all moleculars are dissociated thanks to collisions with the neutral gas, therefore about 99% of the resulting beam is in H_1. The neutralization efficiency at $E_b = 50$ keV is estimated to be 50% for the full energy component, 78% for the E/2 (dissociated H_2^+) and 85% for the E/3 (dissociated H_3^+) beam component [5].

The original particle flux at the ion source (100%) increases due to the dissociation to $1 \cdot 73\% + 2 \cdot 20\% + 3 \cdot 7\% = 134\%$. After neutralisation, approximately 36% of the original flux goes to the full-energy component of the neutral beam, $78\% \cdot 40\% \cong 31\%$ to the half-energy component and $85\% \cdot 21\% \cong 18\%$ to the 1/3 energy component of the resulting neutral beam (at 50 keV). That is, in total some 85% of the particle current gets neutralised. The rest (almost 50% of the original ion source current) is not neutralised, i.e. it is redirected to the ion dump by the DNBI deflecting magnet (see Fig. 1). Notice that the resulting neutral particle flux is usually specified by equivalent current in Amperes.

The beam energy, unlike the particle flux, is conserved, however 50% (H_1^+), 22% (H_2^+) and 15% (H_3^+) of the original power gets not ionised and is lost to the ion dump. Consequently the power in the three neutral beam components equals approx. to 36% (H_1^+), 16% (H_2^+) and 6% (H_3^+) of the total beam power at the source grid.

Due to the beam diffusion the beam edge gets lost to the walls of the DNBI connecting tube or to the diaphragm of the DNBI port. The DNBI technical specifications are met if the neutral equivalent current at full energy which pass through target diameter $r_t = 50$ mm is higher than 0.5 A. Integrating the beam current density at the beam focus (Eq. 1) we get

$$I(r < r_t) = \eta I_{tot}\left(1 - exp\left(-\frac{\alpha r_t^2}{z_{foc}^2}\right)\right) \qquad \text{(Eq. 10)}$$

where I_{tot} is the beam current as measured at the ion source and $\eta \approx 0.36$ for the full energy component of the neutral beam current (see above). For $z_{foc} = 4$ m and the beam divergence $\vartheta = atan(1/\sqrt{\alpha}) = 0.65°$ we get $1 - exp\left(-\frac{\alpha r_t^2}{z_{foc}^2}\right) = 0.70$. From the product of the two factors we can summarize that some 25% of the ion source current go to the target as a full energy neutral beam current, so that the initial current must equal 2 A at minimum. However it is not

clear if all the three beam components have identical beam divergence; the high energy component is probably less divergent so that the resulting beam efficiency may be somewhat better.

4. Beam attenuation in the plasma

Due to collisions between the beam and the plasma particles the beam is attenuated:

$$\frac{dI}{dz} = -\lambda I \qquad \text{(Eq. 11)}$$

or, in an integral form

$$I(B) = I(A)\,exp\left[-\int_A^B \lambda dz\right] \qquad \text{(Eq. 12)}$$

The attenuation coefficient λ is basically given by

$$\lambda v_b = n_e \langle \sigma_e v_e \rangle_b + \sum_j n_j \langle \sigma_j v_j \rangle_b \qquad \text{(Eq. 13)}$$

where v_b is the velocity of the beam particles, the first term on the right describes electron impact ionization and the second term ion impact ionization and charge exchange (summed over all ions species *j*). The collision rate coefficient is strictly defined as

$$\langle \sigma_p v_p \rangle_b = \int \sigma(|v_p - v_b|) f(v_p) dv_p \qquad \text{(Eq. 14)}$$

where $f(v_p)$ is the distribution function of plasma particles *p* and $\sigma(|v_p - v_b|)$ describes the collisional cross-section, which is a function of the plasma-beam particles' mutual speed.

It is clear that the above equations have to be further simplified so that they can be applied in practice. The most important simplification says that the beam particles are much slower that the plasma electrons, and at the same time much faster than the plasma ions:

$$v_j \ll v_b \ll v_e \qquad \text{(Eq. 15)}$$

For example, v_D(500 eV)= 2,2.10^5 m/s, v_b(50 keV)= 3,1.10^6 m/s and v_e(500 eV)= 1,3.10^7 m/s. Thanks to (Eq. 15), we can simply use cross-sections for collisions on ions and zero-weighted rate coefficients for collision on electrons, so that (Eq. 13) simplifies to

$$\lambda = n_e \frac{\langle \sigma_e v_e \rangle}{v_b} + \sum_j n_j \sigma_j \qquad \text{(Eq. 16)}$$

The rate coefficient of the beam particles on the plasma electrons (the electron ionization term) is usually referred as a function of electron temperature so that Maxwellian distribution of electrons is assumed (!). The cross-section of beam-ion collisions (which is only a function of beam energy for $v_b \gg v_j$) should be preferably tabulated under two separate processes: the charge-exchange (CX) and the ionization cross-sections.

Next there is a serious difficulty of sparse knowledge of n_j in (Eq. 16), namely if its dependence on plasma radius (and therefore on the beam coordinate z) is taken into account. In practice one knows from different plasma diagnostics the electron density n_e and the ion effective charge

$$Z_{eff} = \frac{\sum n_j Z_j^2}{n_e} \qquad \text{(Eq. 17)}$$

Luckily enough, it turns out that replacing Z_j/Z_k impurity ions of charge Z_k by an impurity ($Z \neq 1$)of charge Z_j (hence keeping n_e constant) does not change the attenuation considerably [6]. The resonant collisions with hydrogen ($Z = 1$) are substantially more probable. One can therefore reduce (Eq. 16) only to two ion species, deuterium and one (the most typical) impurity element. In other words, all impurity effects can be ascribed to a single impurity species with charge Z.

From the plasma quasineutrality $n_e = n_D + Zn_Z$ and (Eq. 17) we get for the two-species plasma:

$$n_D = n_e \frac{Z - Z_{eff}}{Z - 1} \qquad \text{(Eq. 18)}$$

and

$$n_Z = n_e \frac{Z_{eff} - 1}{Z(Z-1)} \qquad \text{(Eq. 19)}$$

Conclusively, we get from (Eq. 16)

$$\lambda = n_e \left(\frac{\langle \sigma_e v_e \rangle}{v_b} + \frac{Z - Z_{eff}}{Z - 1} \sigma_{totD} + \frac{Z_{eff} - 1}{Z(Z-1)} \sigma_{totZ} \right) \qquad \text{(Eq. 20)}$$

so that for a solution of (Eq. 12) we need knowledge of the following quantities:

- beam initial current and velocity of its particles (derived from beam energy),
- plasma electron density and Z_{eff}(both as a function of beam coordinates, if available),
- the rate coefficient of the beam-electron collisions (as a function of local electron temperature) and the total cross-sections of beam-ion collisions (as a function of beam energy) for two ion species, the deuterium ions and the principal impurity ions,
- hence, we need also plasma electron temperature (as a function of beam coordinates).

The total cross-section consist of charge-exchange cross-section and ionization cross-section: $\sigma_{tot} = \sigma_{CX} + \sigma_i$.

The resulting beam profile in the plasma can be finally described by multiplying the vacuum beam profile (Eq. 6) by an attenuation factor I_z / I_0 which can be derived from (Eq. 12) and (Eq. 20) for any point of the profile.

5. The computer code

For the purpose of the TCV tokamak and its CXR spectroscopy, a set of MatLab functions has been written which models the beam profile and attenuation according to the above derived equations. All the functions, which are described in detail in this chapter, can be found in the / mac/mlynar/matlab/dnbi directory (mac:[mlynar.matlab.dnbi] from VMS machines). A brief help on each function can be, however, found directly from the MatLab command line using *>>help name_of_function*. Within this chapter, we refer to the physical variables by the name of the corresponding MatLab variable rather than by their equation symbols. All input and output values are to be set in SI units.

5.1 Beam vacuum profile

The MatLab function ***vacprof=bevac(zb,rb,Ib,thetab)*** evaluates the vacuum beam intensity according to (Eq. 7) at the position *zb* and radius *rb* respective to the beam axis (*z=0* at the TCV port diaphragm). Optional input parameters *Ib* and *thetab* describe total beam current (at the ion source) and beam divergence, respectively. A set of points can be input at once, i.e. variables z and r can be vectors (of the same length), in which case the output *vacprof* is a vector of the beam intensity at that points. For example, coordinates of points lying on a CXRS viewing line can be input to get the vacuum beam intensity along that line. Notice that the beam components are **not** distinguished within this function; for their description see function ***beat.m*** (section 5.3).

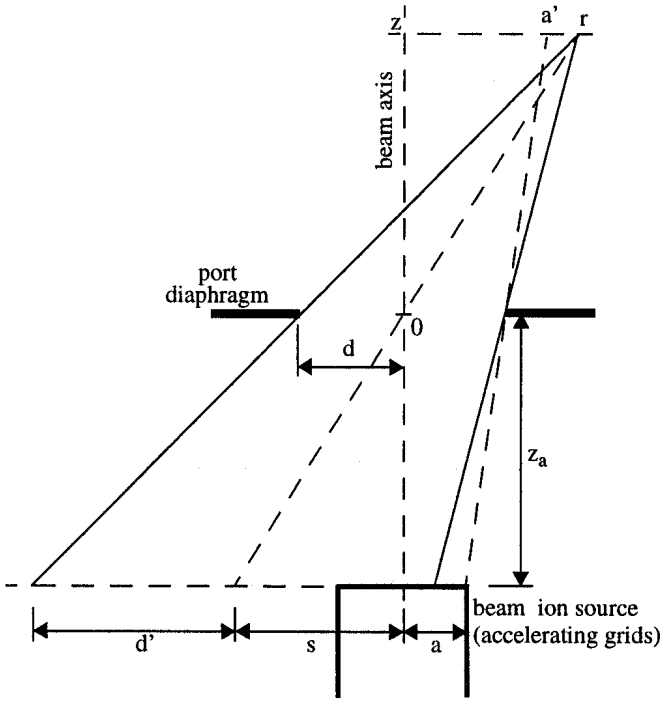

Figure 2: *Geometry of a partial beam source visibility through the TCV port diaphragm.*

The major part of the code deals with the beam source visibility which is limited by the port diaphragm, see Fig. 2. Both the beam source and the diaphragm are supposed to be circular, so that the algorithm evaluates the cross-section surface S_c of two circles: the source's surface πa^2 and the port's projection $\pi d'^2$ (see the figure). The beam profile as given by (Eq. 7) is eventually multiplied by a factor $S_c/(\pi a^2)$.

Default values of the total beam current and the beam divergence are specified at the beginning of the code together with the parameters which specify the beam set-up geometry (z_{foc}, a, z_a, d).

Similarly, the function ***vacprofc=beamprofile(z,Ib,thetab,gc,obsedge)*** finds the vacuum beam intensity profile at the distance z from the ion source by computing the integral (Eq. 5). Optional parameters *gc* and *obsedge* control the form of the output, see the function help. Primary task of this algorithm was to prove that the fast algorithm ***bevac.m*** is fully adequate for our purpose by comparing their outputs *vacprof* and *vacprofc*. This way we could easily verify that their difference is below 10^{-6} within the TCV vessel. However, in case that the beam profile is to be evaluated far from the beam focus - namely in the beam source vicinity - the code ***beamprofile.m*** has to be applied.

5.2 Recovering plasma parameters

The MatLab function ***bedat(shot)*** finds all TCV plasma parameters necessary for the description of the beam attenuation and sets them as global variables. As follows from (Eq. 20), the plasma density *np*, the electron temperature *Te* and the plasma effective charge *Zeff* along the beam are needed. Notice that their time evolution should be known not only at the beam axis but also in the axis vicinity, as steep gradients of density and temperature perpendicular to the beam can occur in TCV, see Fig. 3. As a consequence, the beam profile can be considerably deformed by the plasma, namely in the vertical direction. That is why the function ***bedat.m*** allows to find the necessary parameters along several chords parallel to the beam axis.

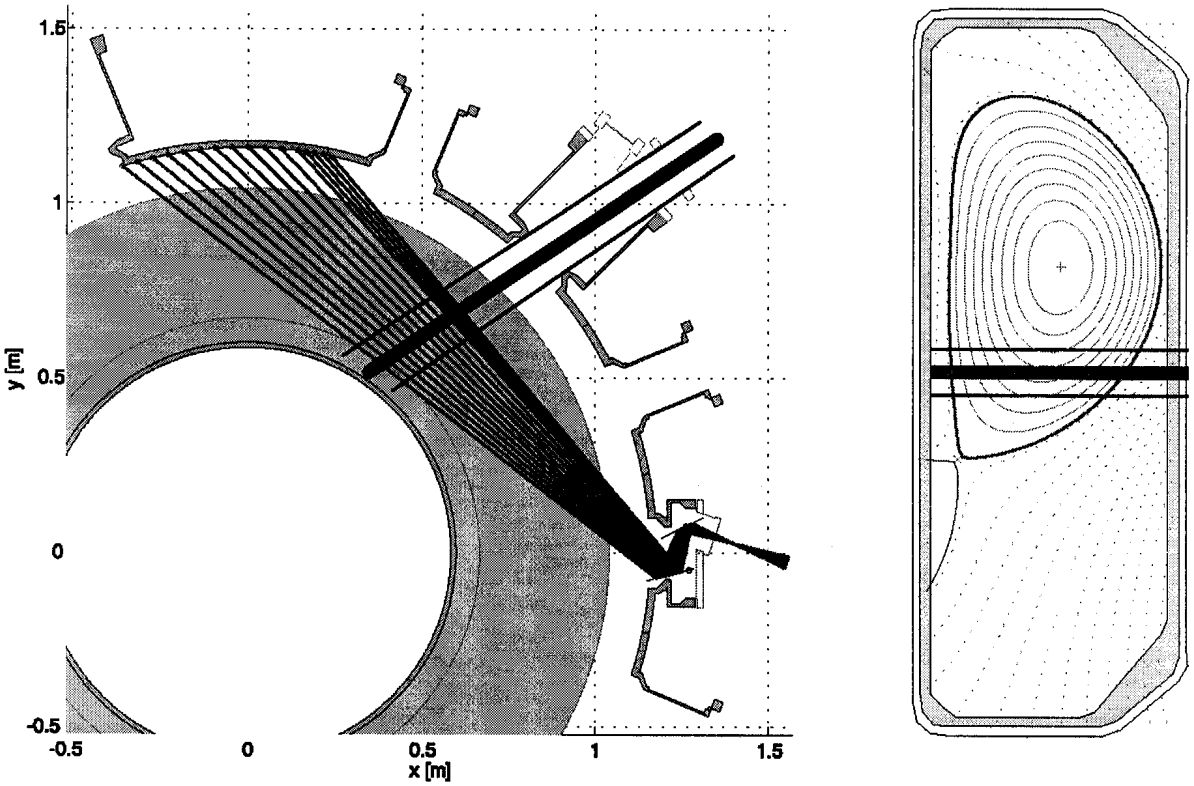

Figure 3: *The beam and CXRS setup vs. plasma geometry in TCV toroidal and poloidal cross-sections,with an example of a real TCV plasma shot (#19594)*

For any TCV shot, both plasma density and electron temperature data can be retrieved in the TCV MDS trees database, which stores their values with 50 ms time sampling rate at 41 flux surfaces (i.e. full poloidal and toroidal symmetry is supposed). The flux surfaces are derived from magnetic reconstruction. Because of limited data available, the effective charge *Zeff* is so far supposed to be constant in space coordinates and only its time dependence is looked for in the MDS trees. If not found, a default constant value of *Zeff* is set up.

After loading the data, the function ***bedat.m*** has to determine density and temperature along the beam in beam coordinate system. TCV can produce strongly shaped plasmas whose position and shape can vary on large scales (see Fig. 3) which considerably complicates geometry of the problem. To handle it we have applied the TCV psi-toolbox for MatLab [7].

The only input of the function is the TCV shot number which is to be analysed. Several global variables allow further specifications:

- *t_min* and *t_max* - the time interval within which the data will be loaded. If the two variables are empty, the whole shot is analysed.
- *x_samp* and *y_samp* - two vectors which set positions of the beam chords along which the density and temperature data will be found. The chords are always parallel with the beam axis, the beam axis has coordinates *x_samp=0, y_samp=0.*

As the output, the procedure ***beadat.m*** sets values of the following global variables:

- *z_samp* which is a *81 x length(x_samp)* matrix. In each column there are 81 coordinates of the psi-toolbox grid (in meters, distance from the port diaphragm), the columns correspond to chords as given by [*x_samp, y_samp*];
- *time* - a vector with sampling times, which are common to *np, Te* and *Zeff*;
- *np* and *Te*, 2-dimensional matrices of size *41 x length(time)* which describe the plasma density and temperature values at the 41 flux surfaces, respectively;
- *npb* which is a 3-dimensional matrix *size(z_samp) x length(time)* and which contains the plasma density data as a function of position and time;
- *Teb* , an analogue of *npb*, 3-d matrix which describe the plasma electron temperature as a function of position and time,
- and *Zeff* which is at present a vector with *length(time)* samples and which describes the average plasma effective charge as a function of time.

5.3 Finding out the beam attenuation

The function ***beamat = beat(shot,Eb)*** finds out the beam attenuation for each of the three beam components at points and times given by the function ***bedat.m*** (see above). The function furthermore specifies details on the three beam components: their initial percentage (73:20:7)[1], the losses in the neutraliser (no losses supposed at present) and the neutralisation efficiency (50:78:85 at E_b = 50 keV). All necessary rate coefficients and cross-sections are loaded from datafile ***beadas.mat*** which has been compiled from the ADAS database.

The ADAS database (dated 1993) supplies total rate coefficients (i.e. electron, ion and charge exchange effects are given unseparated, in one number only). The rate coefficients are classified for eight chemical elements in the SVEN matrix (10x13x8) as a function of 10 different plasma densities (NNE, 10^{18}-10^{21} m^{-3}) and 13 different beam energies (NEB, 5 - 1000 keV), all given

1. All ratios correspond to our knowledge at the release of this report and are subject for later revision.

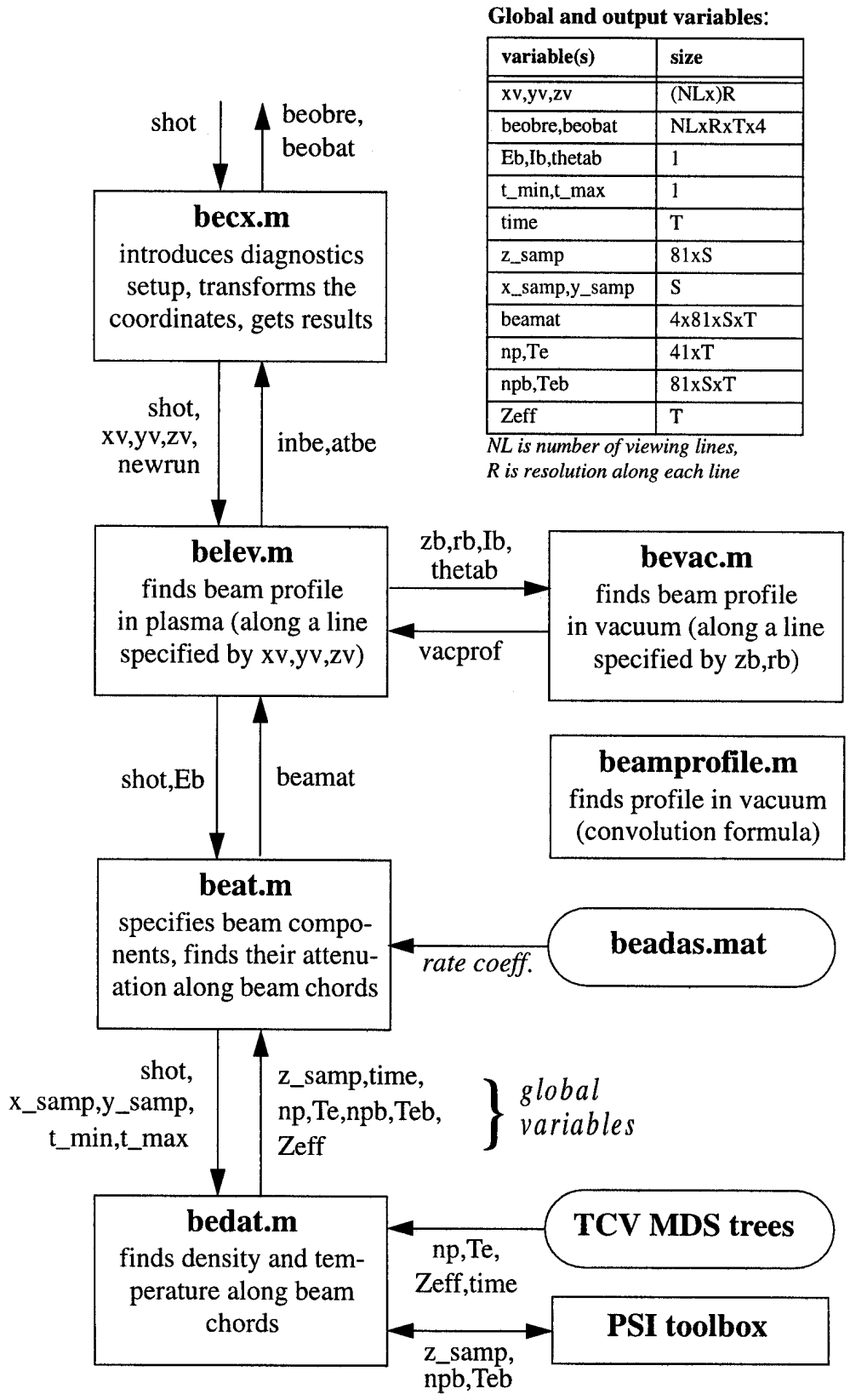

Figure 4: *Scheme of the code package for neutral beam profile and attenuation modelling*

at reference plasma temperature TREF=5 keV. Moreover in matrix SVT the database includes correction rate coefficients for the eight elements at nine temperatures (NTEMP, 0.1-50 keV) at reference beam energy EBREF=50 keV and reference plasma density TREF=5.10^{19} m^{-3}. From these data the function ***beat.m*** interpolates (using splines) the rate coefficients at given beam energy, plasma density and plasma temperature for working gas (hydrogen) and for carbon (Z=6) as the main impurity. The data are then used to determine the attenuation factor from a modified (Eq. 20):

$$\lambda(E_b, c) = n_e(c)\left(\frac{6 - Z_{eff}(t)}{5} \cdot \frac{\langle \sigma v \rangle_{H,\,tot}(E_b, n_e(c), T_e(c))}{v_b} + \frac{Z_{eff}(t) - 1}{30} \cdot \frac{\langle \sigma v \rangle_{C,\,tot}(E_b, n_e(c), T_e(c))}{v_b}\right) \qquad \text{(Eq. 21)}$$

where *c* stands for functional dependence on coordinates, i.e. position and time *(x,y,z,t)*.

It has to be noted that the ADAS database is not optimal for the TCV experiment. Therefore we intend to acquire a database with separated collision effects and with much lower reference temperature (max. 1 keV).

The only inputs of the ***beat.m*** function are the beam shot number and the beam particle energy Eb (full energy component, in keV). The global variables correspond to those in the function ***bedat.m***, see section 5.2. Notice that *t_min, t_max, x_samp* and *y_samp* can be predefined by the user.

The function returns a 4-dimensional matrix *beamat* which describes the beam intensity according to (Eq. 12) as a function of position and time (see global variables *z_samp* and *time*) in the three beam components and in the total beam intensity (which is normalized to 1 at $z = 0$). Consequently, the matrix *beamat* has *(3+1) x size(z_samp) x size(time)* elements.

5.4 Determining the beam intensity along any line

The function ***[inbe, atbe]=belev(shot,xv,yv,zv,newrun)*** finds out the beam intensity (in equivalent Amperes per square meter) in the given *shot* along any colinear points defined by vectors *xv, yv, zv* (in the beam coordinate system, *zv* applies to the beam axis). In other words, it finds the beam profile along a single viewing line. The resulting matrices *inbe* and *atbe* (intensity of beam and attenuation of beam) have three dimensions: *length(xv) x length(time) x 4 (3 beam components & their sum).*

In certain cases the function ***belev.m*** can use the same beam attenuation data *beamat* for the whole set of viewing lines. Repetitive calls of the routine ***beat.m***, which is quite time-consuming, would be redundant then. That is why an optional parameter *newrun* has been introduced. When it is set to zero, the global variables *beamat, z_samp* and *time* are fixed by a single run of ***beat.m*** and once they exist, they are used for any consecutive call of ***belev.m***. An example of *newrun* application can be found in the following section.

As for the principle of the algorithm, ***belev.m*** first selects five points out of the points *xv, yv* and *zv* to define test chords *x_samp* and *y_samp* (unless global variables are predefined). For the five test chords, the function ***beat.m*** is called. Next, the attenuation factor *atbe* is determined for each point *xv, yv* and *zv* by double iteration - first in *z_samp* (attenuation at the projections of the point

onto chords), second in *x_samp* (attenuation at the point itself)[1]. Last, but not in least indeed, the function ***bevac.m*** is called to get the final beam intesity *inbe* as a product of the vacuum beam profile and the beam attenuation factor.

5.5 Example: a fan of viewing lines

The function ***beobre=becx(shot)*** is a realistic example of how to get all beam intensity data for a set of horizontal viewing lines. In this example the viewing lines are supposed to form a diagnostic fan. At the beginning of the function, the geometric setup of the fan is defined as well as its position with respect to the beam, both in the TCV cylindrical geometry. The fan of viewing lines can be even vertically shifted and tilted with respect to the beam axis.

The function ***becx.m*** makes the transformation from the TCV coordinate system into the beam coordinate system and sets the variables *xv, yv* and *zv* which are necessary for the call of the ***belev.m*** function. Within ***becx.m***, *xv, yv* and *zv* are represented by 2-dim matrices (*number of lines x number of sampling points per line*). When the plane of the diagnostic fan is exactly horizontal (i.e. parallel to the beam axis), the parameter *newrun* is set to zero to save the computing time (see section 5.4). The resulting beam intensity is put into the output variable *beobre*, which is 4-dim matrix: *number of lines x size(inbe)*. The corresponding beam attenuation matrix *beobat* as well as the coordinates *xv, yv, zv* can be accessed as global variables. The beam and the plasma characteristics which have been introduced before can be retraced among global variables, too.

* * *

The overview of the code package is presented in Fig. 4. The whole set could be of course fused into a single lengthy code, but we find the present modular form much more practical from the view of future applications. Its total run time at the CRPP hal machine is about 4 seconds for the ***beat.m*** function and one second (per viewing line) for the rest. That is, in the example setup (12 lines) the hal needs 16 seconds for exactly horizontal viewing fan and 60 seconds for a tilted fan.

6. The resulting beam profile and attenuation

In order to illustrate the results of the beam profile and attenuation codes, we examined two shots which have been done during the DNBI tests. Shot #18700 represents a TCV high density plasma (up to 9.10^{-19} m^{-3}), while shot #18705 is a low density one (about $1.6.10^{-19}$ m^{-3}). The plasma has been centered at the beam level (z = 0) in these shots, and time sample t = 0.8 s is considered here. Fig. 5 shows the plasma electron temperature and density along the beam axis as well as the on-axis (peak) beam intensity. Beam attenuation in the two cases can be easily compared to the unattenuated beam intensity in vacuum. Notice that even in vacuum there is certain decrease in the beam on-axis current density due to the beam divergence.

The same comparison is presented in Fig. 6 for the beam profile, i.e. for the beam intensity perpendicular to the beam axis. The dashed line corresponds to the beam focus, though it may not seem so due to beam divergence (see the vacuum case, Fig. 6a).

---

1. Special care has been devoted to a compact, matrix form of the iteration algorithm. As compared to the standard, simple form of a separate iteration run per each matrix dimension, the compact form of the algorithm has been found 10 times (!) faster.

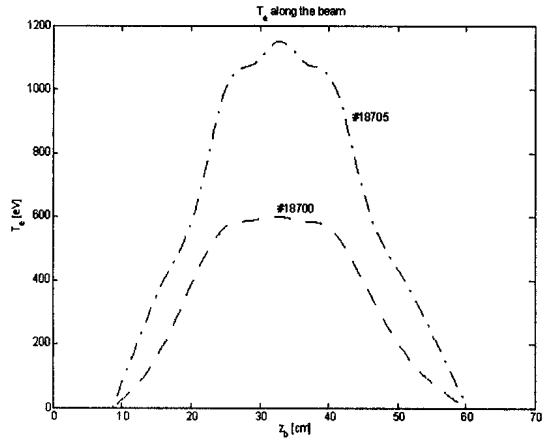

a.

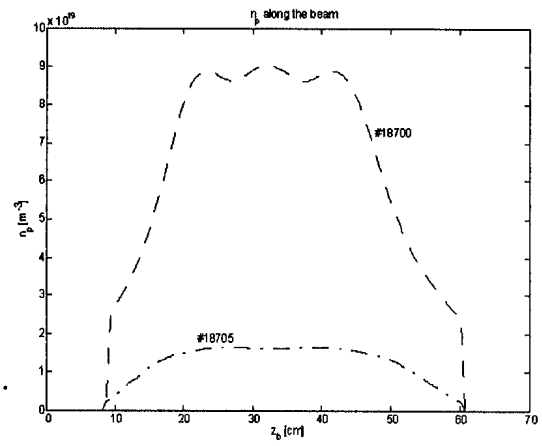

b.

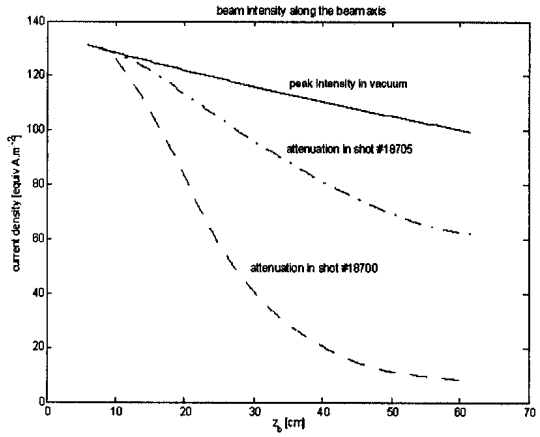

c.

Figure 5: *plasma parameters and corresponding beam attenuation along the beam axis.* ***a*** *- plasma electron temperature,* ***b*** *- plasma density,* ***c*** *- resulting beam intensity.*
dashed line - shot #18700 at 0.3s
dash-dot line - shot #18705 at 0.3s
full line - beam intensity in vacuum

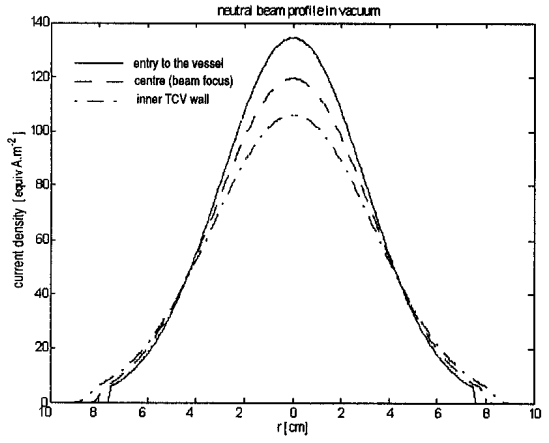

a.

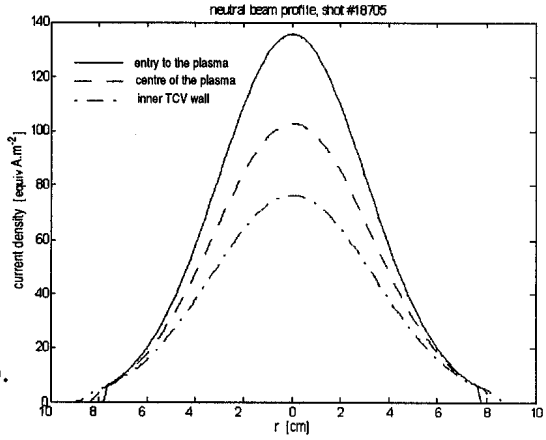

b.

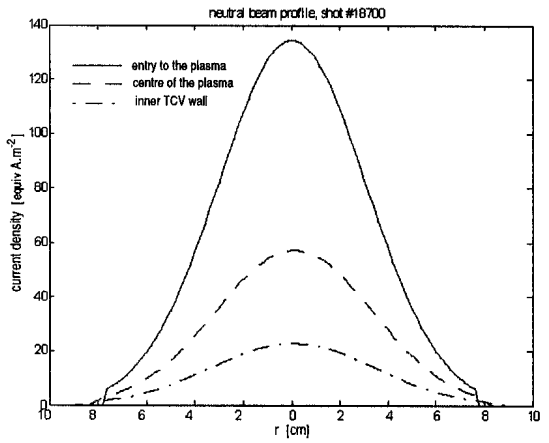

c.

Figure 6: *neutral beam profile* ***a*** *- in vacuum (pure beam divergence),*
b *- shot #18705,* $n_p \sim 1.6 \cdot 10^{19} m^{-3}$,
c *- shot #18700,* $n_p \sim 9 \cdot 10^{19} m^{-3}$,
full line - initial beam profile
dashed line - beam profile in focus
dash-dot line - beam profile at TCV inner wall

Further, a special set of computations has been performed to obtain a realistic model of beam attenuation as a function of density and beam energy. The plasma transparency to the beam as a function of plasma density (Fig. 7) has been traced for plasma characteristics as given by shot #18705 (but for a multiplication factor to n_p). The result illustrates that the beam attenuation is strongly dependent on plasma density. At the same time it can be clearly seen that the beam characteristics correspond well to the TCV plasma parameters, about a half of the beam intensity is lost under standard TCV conditions, which is desirable for the beam diagnostics. Notice that the ion source intensity is taken as the initial intensity, of which only 85% goes to neutral beam (see section 3).

The plasma transparency to the beam as a function of available beam energies is presented in Fig. 8 for the low and high density plasma shots. It turns out that the beam energy is not primary for the attenuation. Taking into account the fact that the beam has been optimized for E_b = 50 keV and that its performance (namely its total current) decreases with the particle energy, this result supports our general view that the beam need not be operated for energies lower than 50 keV.

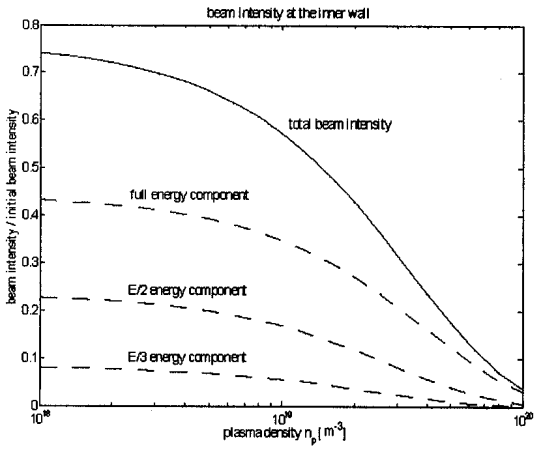

Figure 7: *Plasma transparency to the beam as a function of plasma density (full line - total beam intensity, dashed lines - individual beam components)*

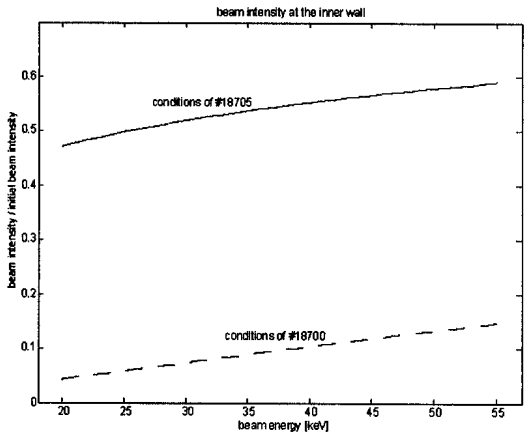

Figure 8: *Plasma transparency to the beam as a function of beam energy. Full line - low density shot #18705, dashed line - high density shot #18700*

7. Conclusions, acknowledgements

A flexible model of diagnostic neutral beam profile and of its attenuation in plasma is necessary for absolute CXRS measurements, which we intend to realize at TCV tokamak. This work has put all necessary groundworks for such a model. A trustworthy profile approximation has been derived in (Eq. 6) and (Eq. 7). Beam components have been discussed quantitatively in section 3. An approximative formula for the beam attenuation which requires only data available in the present TCV MDS trees has been presented in (Eq. 20).

A package of MatLab codes for the DNBI profile and attenuation evaluation has been presented, see Fig. 4. It calculates on variable geometries of the TCV plasmas and still is fast enough so

that the voluminous output results need not be saved. At present the code package includes neither the halo effect nor the iterative feedback to the impurity concentration effect on the beam attenuation, but it has been written in modules to allow for any further extension. In a similar way, any new database of rate coefficients (and/or cross-sections) can replace the present ADAS database, which does not suit well the TCV needs. Finally, a module with all necessary emission data is to be included according to needs of CXRS diagnostics to determine the impurity radiation from the beam intensity level.

The author would like to acknowledge the support of both CRPP and BINP groups. My personal thanks go to Prof. A.A.Ivanov from BINP Novosibirsk for his numerous remarks on beam profile and components and to Paolo Bosshard for his considerable help with the ADAS database reading.

This work was partly supported by the Swiss National Science Foundation.

8. References

[1] P. Bosshard: Présentation et étude de performances du diagnostic CXRS sur TCV
INT 201/01 (in French, CRPP EPFL 2001)

[2] M.G. von Hellermann, H.P.Summers: Active Beam Spectroscopy at JET
JET-P(93)34 (Abingdon, 1993)

[3] A.A. Ivanov et al.: Radio Frequency Ion Source for Plasma Diagnostics in Magnetic Fusion Experiments, Rev.Sci.Instrum. 71, 3728 (2000)

[4] B.P. Duval: Spectroscopic studies of highly ionised atoms, ch. 3.7.5
(doctoral thesis, Oxford 1986)

[5] A.A. Ivanov, BINP Novosibirsk, private communication

[6] I.H. Hutchinson, Principles of plasma diagnostics, ch. 8.2.1
(Cambridge University Press, Cambridge,1987)

[7] J.-M. Moret, The TCV Psi-Toolbox tutorial
http://crppwww.epfl.ch/~moret/psitbx/psitbxdemo.html